Available online at www.sciencedirect.com
SCIENCE DIRECT®
ELSEVIER
Journal of Crystal Growth 249 (2003) 354–362
JOURNAL OF CRYSTAL GROWTH
www.elsevier.com/locate/jcrysgro

Process from monodispersion to regular aggregation in Duck Cu, Zn superoxide dismutase crystallization observed by atomic force microscopy

Genpei Li[a,b], Jianwei Li[c], Chunli Bai[c], Da-Cheng Wang[a,b,*]

[a] *Institute of Biophysics, Center for Molecular Biology, Chinese Academy of Science, Beijing 100101, China*
[b] *National Microgravity Laboratory, Chinese Academy of Science, Beijing 100080, China*
[c] *Institute of Chemistry, Chinese Academy of Science, Beijing 100080, China*

Received 13 June 2002; accepted 10 October 2002
Communicated by R. Giegé

Abstract

Up-to-date, considerably less is known about the early stage in protein crystallization. By using AFM a stepwise process from the solution state to the regular aggregation in the early stage of Duck Cu, Zn superoxide dismutase (dSOD) crystallization has been observed. The process could be divided into four steps. At the beginning dSOD is in monodispersion as dimers. As supersaturation increases the irregular aggregation gives rise to linear polymers with different sizes and branches. When the system is nearing the maximum supersaturation the partial regular oligomerization happens to produce the oligomers with limited size, basically the nonamers of dSOD. In about 20 days after setup of the experiment regular assemblies with a double-helix-like pattern emerge from solution. Then the single crystals grow in about 45 days. The X-ray crystallographic analysis shows that the unique packing unit in the crystal is a double-helix formed by two strands of dSOD nonamers with 9_2 screw symmetry, which is well corresponding to the observation in the AFM images. The observations provide the experimental information for a better understanding of the process from solution to nucleation in protein crystallization.

PACS: 81.10.aj

Keywords: A1. Atomic force microscopy; A1. Biocrystallization; A1. Nucleation; B1. Proteins

1. Introduction

The crystal growth process of proteins can be divided into discrete stages, including nucleation, crystal growth, and cessation of growth. Nucleation is the early stage and prerequisite for the growth process of crystals. Therefore, it is crucial for understanding the crystallogenesis of proteins.

*Corresponding author. Institute of Biophysics, Center for Molecular Biology, Chinese Academy of Science, 68, 15 Datun Road Chaoyang District, Beijing 100101, China. Tel.: +86-10-6488-8547; fax: +86-10-6488-8560.
E-mail address: dcwang@sun5.ibp.ac.cn (D.-C. Wang).

0022-0248/03/$ - see front matter
PII: S0022-0248(02)02059-6

Although a great deal is known about bulk crystals, considerably less is known about their early stage, when they nucleate and grow from a liquid. The nucleation events have been widely investigated and thoroughly analyzed by many techniques, such as light scattering [1–4], small angle X-ray scattering [5,6] and neutron scattering [7], and computer simulation [8] as well. However, the nature of the nucleus and the process by which the critical nuclear size is attained are still a mystery [9,10]. Especially, attempts to distinguish the amorphous aggregates from the structuralized aggregates with these techniques are hampered by the lack of experimental observations to show the process from monodispersion to regular aggregation in prenucleation, the early stage of protein crystallization. Recently, a novel technique, atomic force microscopy (AFM), has been effectively used in studying the mechanism of crystal growth [11,12]. In this paper we will report a stepwise process from the monodispersive molecules to the regular aggregate with a double-helix pattern observed by AFM in the early stage of crystallization of Peking duck Cu, Zn superoxide dismutase (dSOD).

dSODs are the essential metalloenzymes from a particular bird, the Peking duck. The Peking duck (*Anas platyrhynchos domestica*) is a domestic species of *A. platyrhynchos,* who compulsively consumes much more than they physiologically require. Despite their excessive obesity compared with other duck species, Peking ducks rarely suffer from cardiovascular and cerebrovascular diseases such as atherosclerosis and hypercholesterolaemia [13]. Efforts have been made to determine the effective factors in this phenomenon. In view of the close relationship between lipid peroxidation and atherosclerosis as well as aging, through investigation of dSOD, including the 3D structure, becomes of particular interest. As the first step, the crystallization was carried out. The growth of dSOD crystals and the preliminary X-ray analysis showed some special features. Firstly, the crystal growth rate is very slow. It usually takes about 7 weeks to grow a perfect crystal. Secondly, as an unique structural unit, an unusual supramolecular assembly with a double-helix pattern and $9_2 2$ non-crystallographic symmetry has been observed in crystals [14]. Besides, dSOD exists in solution as dimers. With these favorable conditions, we try to use this system to trace the prenucleation process in the early stage of crystallization. The studies reported in this article have provided a direct visualization and evidence for the existence of dSOD regular aggregates during the process of prenucleation through the molecular self-assembly.

2. Materials and methods

2.1. Sample and chemicals

The dSOD molecules consist of 308 residues with MW 16 kDa. They are dimeric in solution usually. The samples of dSOD used in the experiments were prepared from fresh duck blood in our lab. The procedures of purification and characterization have been described in previous report [14]. The dSOD dry powder was dissolved in cacodylate buffer (pH 6.8) at 60 mg/ml and stirred 3 min, and then centrifuged for 15 min at 10 000 rpm. All chemicals used in the present study were of analytical grade and used without further purification, but all solutions were subsequently filtered with a micro-filter with a ϕ 0.22 μm before use.

2.2. Crystallization setup and working solution

The crystallization trials for the experiments, using sitting drop vapor diffusion, were setup as described previously [14]. Briefly, the stock solution of dSOD was mixed with an equal volume of crystallization medium containing 30% (v/v) of MPD, 19% (v/v) of hexane-1,6-diol in 0.01 M cacodylate buffer at pH 6.8. Under this condition, the crystals were grown in trigonal space group $P3_221$ with unit cell parameters $a = 125.4$ Å, $c = 163.3$ Å $\gamma = 120^\circ$. Crystals, typically, with dimension of $0.2 \times 0.2 \times 0.8\,mm^3$, grew in about 6 weeks at 7°C (see Fig. 2a).

The working solutions for AFM experiment were sampled 1 μl of the mother liquor from crystallization drops setup by 5 days of interval, i.e. 5, 10, 15, and 20 days, respectively. The

relevant concentrations of the dSOD enzyme were measured with the standard calibrated curve with interpolation method, and the calibrated curve made from the UV absorbance at a wavelength of 280 nm. The concentrations can be also measured using an Abbe's refractometer calibrated with β-monobromonaphthaline and pure water refractive index ($nD = 1.6666$ and 1.3333). The supersaturation β is defined as the ratio of the actual concentration C over the equilibrium concentration (i.e. the solubility of the dSOD enzyme) at the crystallization temperature.

2.3. Acquisition of AFM images

All AFM samples were prepared by injecting 1 μl of the working solution into a 20 μl droplet of buffer solution on a freshly cleaved mica support surface. After a 10 min incubation, excess moisture was removed by wicking with the edge of a piece of filter paper until only a thin film of solution remained on the substrate, then air-dried for approximately 15 min in a humid chamber. Each sample was blown out with N_2 gas before transferred to the AFM stage. It is known from the previous crystallization experiment that the micro-crystals could appear within about 3 weeks under the crystallization conditions. We therefore believed that it is possible to capture the formation of the various aggregates within the nucleation time scale by using this mean. A NanoScope III controller with a Multi-Mode AFM head (Digital Instruments, Santa Barbara, CA, USA) was used to image the above samples. All observations were made in air at 13°C and a relative humidity of about 40% by operating the height and deflection modes with spring constant of about 0.8–1.8 nN and a scanning rate of 1.5–4 Hz for a range of resolution. No image smoothing or noise removal was carried out.

In order to exclude the possible artifacts the AFM system was tested in various steps with control, including repeating the scan, changing the scan direction, scan size, scan speed and the orientation of the sample. In addition, some blank tests containing buffer and precipitants only were carried out before start of the data acquisition.

2.4. X-ray crystallography

With the same setup and conditions as described above, the crystallization was carried out. The crystals of dSOD were grown up in about 45 days. The X-ray diffraction data collection and the preliminary crystallographic analysis were performed as previously described [14].

3. Results

The AFM images of dSOD in different degrees of super saturation ($\beta = 4$–7.8) with time evolution were routinely obtained and shown in Fig. 1. The images were permitted to trace the process from monodispersion to regular aggregation at a molecular-level contrast. Fig. 1a shows the state at the beginning (0–5 days) of dSOD crystallization under the unsaturated conditions, $\beta = \sim 4$. The image clearly revealed the dSOD dimers, as detected at this stage, existing as discrete ellipsoids or spheres with an apparent dimension of about $24 \times 45\,\text{nm}^2$ (average size of ~ 35 nm). This observation experimentally showed a monodispersive state of dSOD dimers as predicted by many

Fig. 1. AFM images showing the stepwise process from monodispersion to regular aggregation in the early stage of dSOD crystallization. Images are acquired in Tapping Mode with a scan rate of approximately 1.0–1.8 Hz. All observations were performed in air at a humidity of approximately 40%. (a) An image of dSOD dimers in the mother liquor solution at the initial stage of crystallization ($t = 5$ d, $\beta = \sim 4$). The discrete ellipsoids observed in the image show the monodispersion of dSOD dimers in undersaturation. The size of the dSOD dimer in AFM images appears much larger than in real size due to the dependence on the geometrical shape and size of the tip used for imaging. (b) Image of dSOD aggregates after 10 days of crystallization ($\beta = 6.8$). Unregular aggregation can be seen at this stage. (c) Image taken after 15 days and near the maximum oversaturation ($\beta = 7.8$). The dSOD aggregates become partially regular with limited size. (d) Close-up view of a typical oligomer highlighted in (c) corresponding to a nonamer of dSOD dimer. (e) A regular aggregate with a double-helix-like pattern appeared in 20 days at oversaturation suitable for crystallite emergence ($\beta = 7.0$). The assembly shown in the image may consist of 300–400 dSOD dimers.

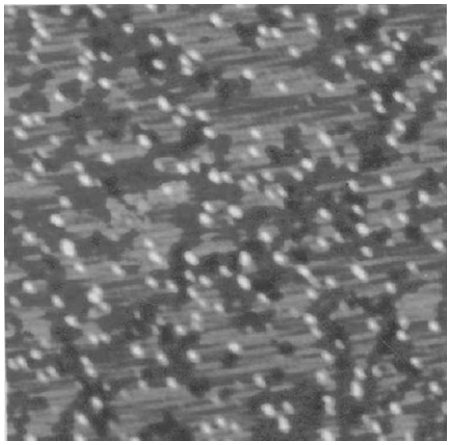

(a) Scan size: 1×1 μm^2

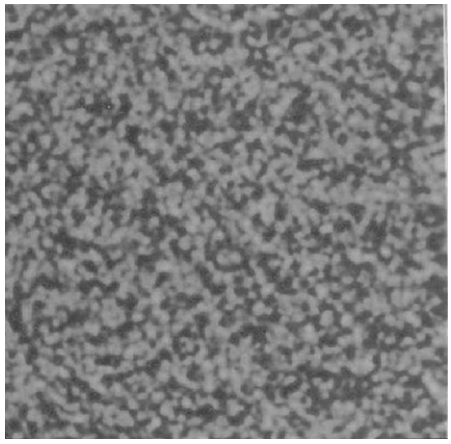

(b) Scan size: 1×1 μm^2

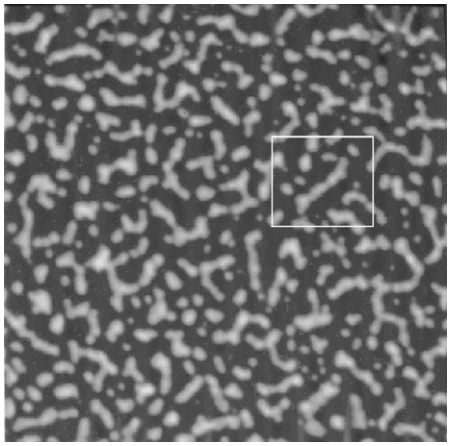

(c) Scan size: 1×1 μm^2

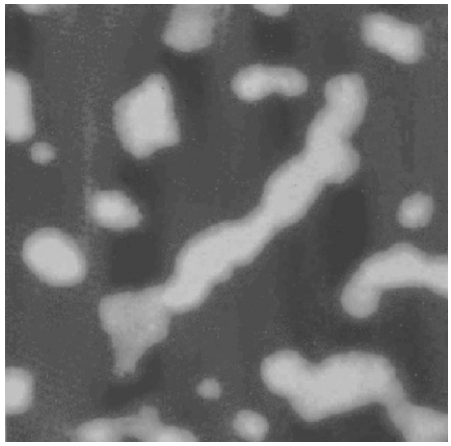

(d) Scan size 200×200 nm^2

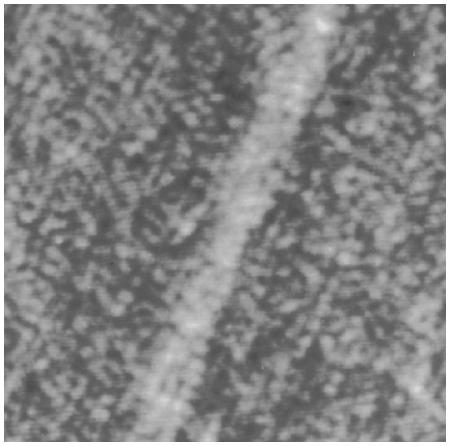

(e) Scan size: 800×800nm^2

investigations with other techniques (e.g. [15–18]). It indicated that monodispersity of molecules in solution seems to be a prerequisite to crystallization.

With the increase of supersaturation, the monodispersive dSOD dimers start to aggregate. Fig. 1b shows the AFM image taken after 10 days (β value estimated as about 6.8), from which a large number of dSOD aggregates are observed. The random sizes and various shapes of the aggregates indicated that the aggregates at this stage were nonregular and the formed polymers were mainly in spatially disorder. As time goes on and the supersaturation increases the dSOD aggregates become more or less regular. Fig. 1c was taken at the 15th day after the setup, where the β value reached about 7.8, near the maximum supersaturation of the system. Most of aggregates appeared in the image are linear oligomers with limited size. A typical one is a single strand aggregate with a length of 150–180 nm (Fig. 1d). When it came to the 20th day, a double-helix-like assembly appears in the AFM image as shown in Fig. 1e. The estimated β value for this image was about 7.0. Interestingly, the crystallization experiment showed that the crystallites of dSOD also appeared in this period, about three weeks after setting up of the solution droplet for the crystallization.

The molecular packing in the dSOD crystal and its architecture elucidated by X-ray crystallographic analysis confirmed the AFM observations on the regular aggregate and further revealed the detailed structure of the double-helix-like assembly seen in the AFM image. In the parallel experiment with the same recipe, dSOD molecules crystallized by using the sitting-drop vapor-diffusion method. The details about the crystallization, data collection and preliminary X-ray analysis were described in a previous report [14]. The diffraction-quality crystals grew in about 7 weeks and diffracted to a 2.9 Å resolution. The dSOD crystals (Fig. 2a) are trigonal with space group $P3_221$ and cell parameters $a = 125.4$ Å, $c = 163.3$ Å and $\gamma = 120^\circ$. They are mostly long needle-like and easy to split into thinner needles along the longitudinal direction. The preliminary structural analysis has shown unusual molecular packing. 24 dimeric dSOD molecules in a unit cell are packed as two interwinding helices with a 9_22 non-crystallographic symmetry and form a supramolecular double helix in the trigonal crystals. The six adjacent double helices generate a hexagonal channel along the c-axis. A schematic view of this unique packing is depicted in Fig. 2b. The unique double helix is characterized by a nonamer unit $\sim(D_1–D_2–D_3–D_9)_n\sim$ (D = dSOD dimer), in which each dimer is related to each other by a rotation 40° about the helix axis and translation 3.63 nm along the axis. In such a way, two strands of this nonamer unit interwind into a turn of the double helix with a axial periodicity of 32.6 nm, just twice of c-axis, as shown in Figs. 2c and d.

In association with the packing and quaternary structural information in the dSOD crystals revealed by X-ray crystallography, the AFM observation could be interpreted in more details. In the process from the monodispersive dSOD dimers to the rather regular aggregate, the linear assemblies should basically consist of the nonamers of dSOD (Figs. 1c and d). However in this stage, interactions between the dSOD dimers are restricted in a limited single area of the molecules due to the linear aggregation, which may not be enough to stabilize the aggregates to keep a regular form. In fact, the components emerged in the image are variant in different sizes. Evidently, the double-helix-like aggregates observed in AFM image (Fig. 1e) should correspond to the unique double helix consisted of two strands of the dSOD nonamer assemblies found in dSOD crystals. Though the quaternary structural details of this double-helix aggregate could not be measured from the AFM image at the moment, it is plausible to infer that the characterization of these aggregates are similar to that observed in dSOD crystals. The dimension of this regular aggregate is about 780 nm as measured from the AFM image, which correspond to about 20 double helices (the periodicity of a helix is 32.6 nm) and 300–400 dSOD dimers. Furthermore, through the double helix, a regular pattern of interactions is formed. Therefore, the aggregates at this stage are energetically favorable. These double-helix aggregates should be the basic unit for the dSOD assembly in the crystal growth.

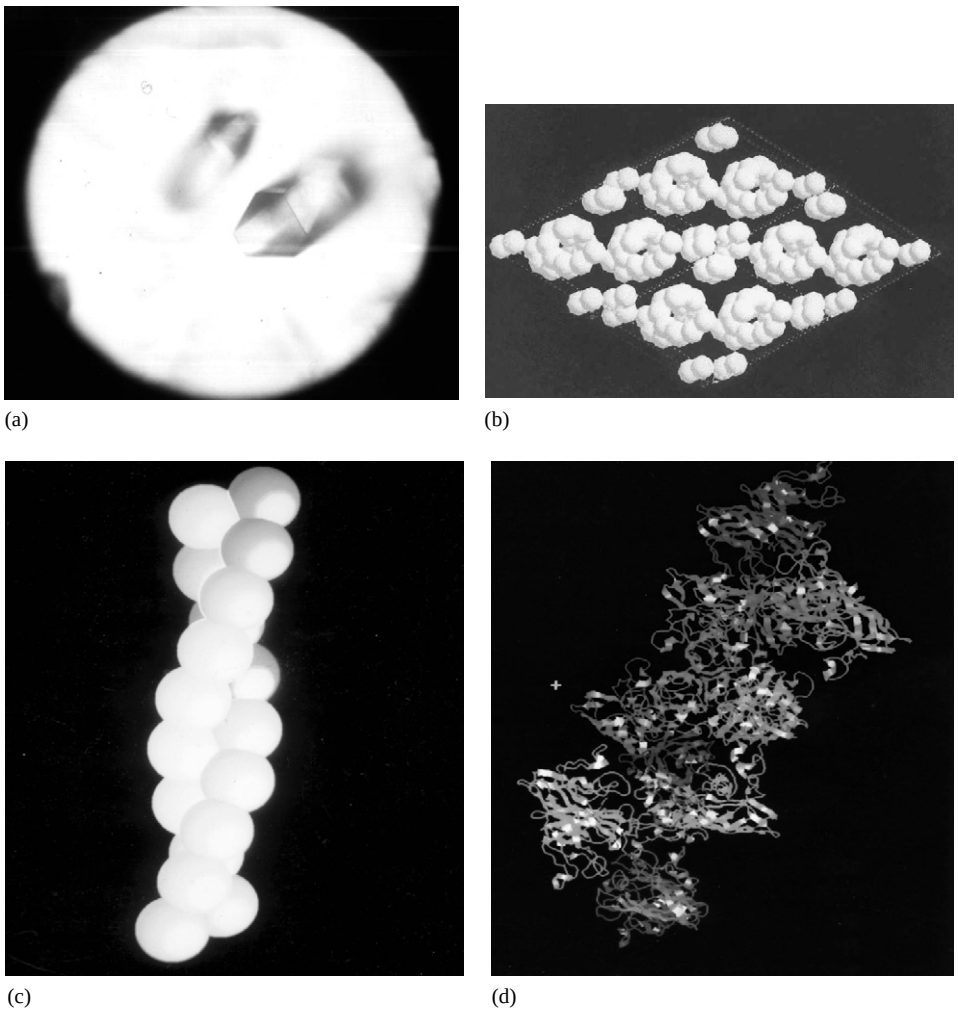

Fig. 2. A typical dSOD crystal and the crystal architecture revealed by the X-ray crystallographic analysis. (a) Crystals with space group P 3_221 growing in about 45 days with the same recipe as in the AFM setup. (b) Molecular packing in the trigonal crystals. Two interwinded helices with a 9_22 non-crystallographic symmetry form a supramolecular double helix. Eight unit-cells oriented along *c*-axis in vertical are shown in the figure. In this area each stretch have a helical period. Spheres represent dSOD dimers. (c) The schematic view of a period of the dSOD double helix in which each strand consists of nine dSOD dimers related each other by 9_2 screw symmetry. The assembly of this double helix based on dSOD nonamers corresponds well to the double-helix-like assembly observed in the AFM image (see Fig. 1e). (d) Ribbon representation of dSOD molecules assembled as in (c) revealed by the preliminary X-ray structural analysis.

4. Discussion

Though quite a lot of works has been done for investigating the nucleation in crystallization of proteins, the questions about nature of the nucleus and the process to form the nucleus are still open (see reviews [9,10,18]). In this work AFM images in association with X-ray crystallographic analysis revealed the process from a monodispersion to a regular aggregation in dSOD crystallization. The most interesting finding is that the regular aggregation, a double-helix-like oligomer, observed by AFM (see Fig. 1e), is correspond well to the basic structure, a double helix with a

9_2 non-crystallographic symmetry (see Figs. 2b and c), packing in the crystals. If we refer to the emergence of crystalline order as nucleation, these double-helix-like aggregates of dSOD can be considered as the pre-nuclei or even the nuclei formed in the early stage of dSOD crystallization. In fact, these aggregates contain at least 300–400 molecular units, which are large enough to be stabilized by a number of intermolecular interactions. Meanwhile the regular pattern of interactions is also formed through the double-helix pattern assembly. All these have fit to the basic conditions of a nucleus as suggested by some detailed analysis. In the case of dSOD crystallization this nucleus seems structurally in order.

In association with a curve showing the dependency of protein concentration on times in dSOD crystallization [19], the process from the monodispersive state to the regular aggregation and the crystal growth are schematically shown in Fig. 3. Different from the one-step or two-step nucleation mechanism [20, 21], the process observed in this work is stepwise, containing mainly four steps. In the first stage ($t = 0-5$ days, $\beta = \sim 4$), dSODs are monodispersive as shown in Fig. 1a. The monodispersive unit is dSOD dimer as it is in solution. A series of reports (e.g. Refs. [17,18,22]) have shown that monodispersity of molecules in solution seems to be a prerequisite to crystallization even in supersaturated solution. Therefore, the monodispersive dSOD dimers are the basis for evolving regular aggregates. As supersaturation increases, dSOD molecules spontaneously aggregate in unregular way (Fig. 1c). In this stage the aggregates are mainly linear polymers with different size and pattern and the intermolecular interactions are not specific. When the supersaturation is near the extreme condition ($\beta = 7.8$, $t = 15$ days), the partially regular oligomerization gives rise to linear oligomers of single strand with limited size (Figs. 1c and d). The basic unit of these oligomers corresponds to a nonamer of dSOD dimers. This organization has shown partial regularity. However, it is not steady because there are not enough molecules for molecular aggregates and it, especially, lacks a specific pattern of intermolecular interactions. In fact, these small aggregates appeared in the AFM image are not uniform

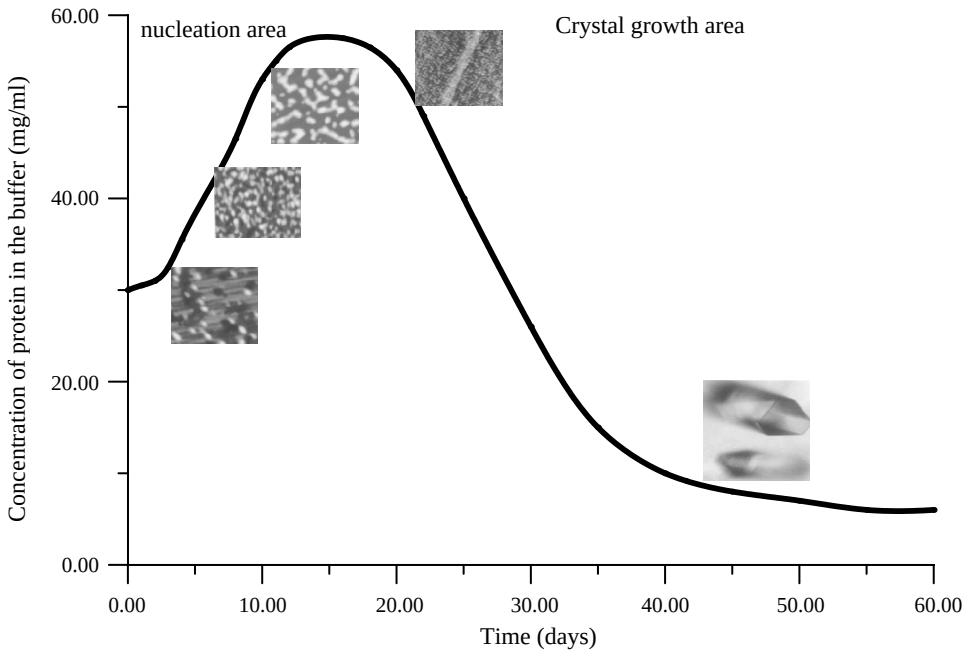

Fig. 3. Time-concentration profile in correlation with the process from monodispersion to regular aggregation and crystal growth in dSOD crystallization. The time-concentration curve was previously measured [19].

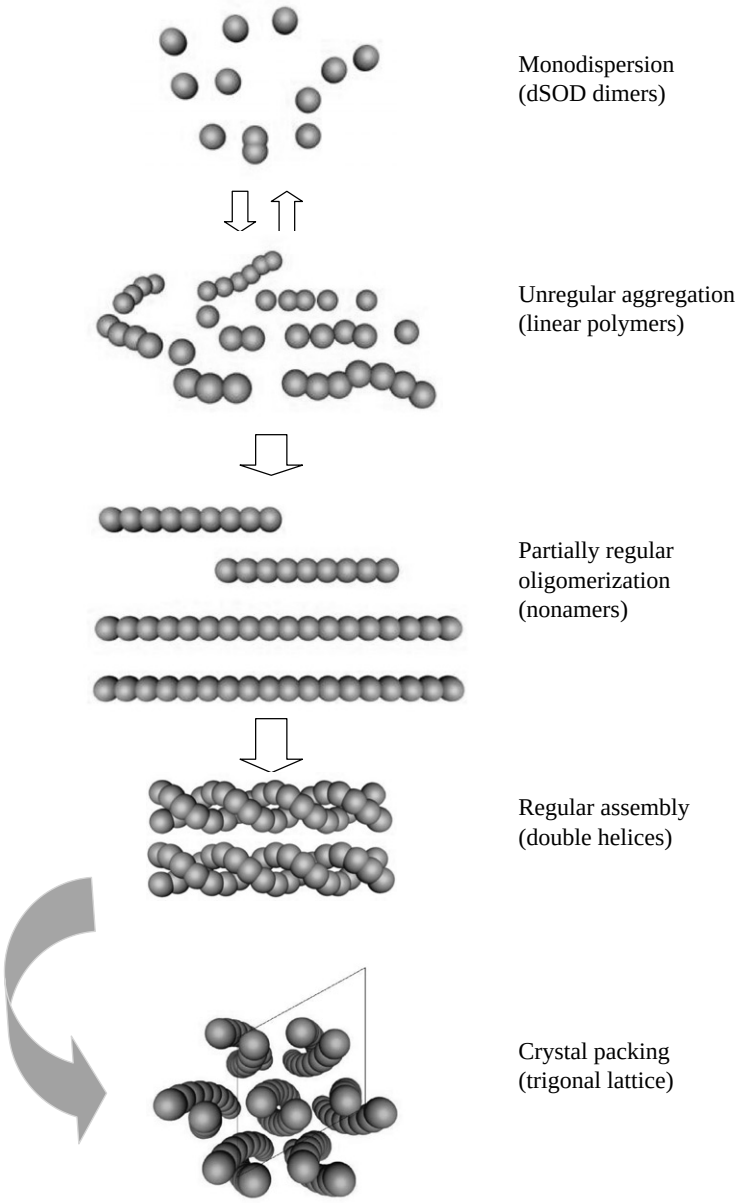

Fig. 4. Schematic representation for the stepwise process in dSOD crystallization suggested by AFM observation and X-ray crystallographic analysis.

(Fig. 1d). In the next stage these linear oligomers further associates through specific interactions to form a regular coiled-coil pattern, which is corresponding to the double-helix assembles in crystals (Figs. 1e and 2c). Formation of these regular aggregates is energetically favorable and large enough to be stable. It seems that the formation of the regular aggregates with the double-helix pattern may promote the nucleation process and constitute an energy barrier to

crystallization. In this stage the concentration has begun to be reduced. It is plausible to assume that the process was fallen into the area of the nucleation at the end of this stage. The last stage includes the process of crystal growth, in which the regular assemblies with the double-helix pattern further adhere and pack to form a trigonal crystal.

The four steps from the monodispersion of dSOD dimer to the regular aggregates with double-helix pattern are schematically shown in Figs. 3 and 4. Referring to the main features of a nucleus [9, 10], the dSOD double-helix-like aggregates emerging in the third stage could be considered as prenuclei or even nuclei in dSOD crystallization because they generally fit to the basic prerequisite for a nucleus.

Acknowledgements

We are indebted to Professor W.R. Hu for his continuous encouragement during this work. This work was supported by the Basic Research Program (95-Yu-34) from the Ministry of Science and Technology of China and Chinese Academy of Sciences.

References

[1] G. Feher, Z. Kam, Methods Enzymol. 114 (1985) 77.
[2] A.J. Malkin, A. McPherson, J. Crystal Growth 128 (1993) 1232.
[3] W. Kadima, A. McPherson, M.F. Dunn, F. Jurnak, J. Crystal Growth 110 (1991) 188.
[4] M. Muschol, F. Rosenberger, J. Chem. Phys. 103 (24) (1995) 10424.
[5] F. Boué, F. Lefaucheux, M.C. Robert, I. Rosenman, J. Crystal Growth 133 (1993) 246.
[6] S. Finet, F. Bonneté, J. Frouin, K. Provost, A. Tardieu, Eur. Biophys. J. 27 (1998) 263.
[7] F. Bonneté, O. Vidal, M.C. Robert, A. Tardieu, J. Crystal Growth 168 (1996) 185.
[8] M. Pellegrini, S.W. Wukovits, T.O. Yeates, Proteins Struct. Funct. Genetics 28 (1997) 515.
[9] A. McPherson, Yu G. Kuznetsov, A. Malkin, Structure 3 (1995) 759.
[10] G.L. Gilliland, J. Ladner, Curr. Opinion Struct. Biol. 6 (1996) 595.
[11] S.D. Durbin, W.E. Carson, J. Crystal Growth 122 (1992) 71.
[12] A. McPherson, A.J. Malkin, Yu G. Kuznetsov, M. Plomp, Acta Cryst. D57 (2001) 1053.
[13] P. Ye, B. Chen, S. Wang, Atherosclerosis 117 (1995) 43.
[14] Liu Wei, Li Pingwei, Genpei Li, Rong-Huan Zhu, Da-Cheng Wang, Acta Cryst. D57 (2001) 1646.
[15] M. Zulauf, A. ĎArcy, J. Crystal Growth 122 (1992) 102.
[16] V. Mikol, E. Hirsch, R. Giege, J. Mol. Biol. 213 (1990) 187.
[17] S. Veesler, S. Marcq, S. Lafont, J.P. Astier, R. Boistelle, Acta Cryst. D50 (1994) 355.
[18] Yu.G. Kuznetsov, A.J. Malkin, A. McPherson, J. Crystal Growth 196 (1999) 489.
[19] P.W. Li, Ph.D. Dissertation, Peking University, 1996.
[20] J. Drenth, C. Haas, Acta Cryst. D54 (1998) 867.
[21] C. Haas, J. Drenth, J. Crystal Growth 196 (1999) 388.
[22] F. Thibault, J. Langowski, R. Leberman, J. Crystal Growth 122 (1992) 50.